Romanian Journal of Petroleum & Gas Technology
Vol. V (LXXVI) • No. 2/2024

MODELING OF THE ZONES OF INFLUENCE OF GAS WELLS AT A DEPLETED RESERVOIR

Ioan Alexandru Stoica [1,3 *]

Lazăr Avram [2]

Bogdan Simescu [1,3 *]

Mihaela Helstern [4]

[1] Petroleum and Gas Doctoral School, Petroleum-Gas University of Ploiesti, Romania
[2] Faculty of Petroleum and Gas Engineering, Petroleum-Gas University of Ploiesti, Romania
[3] ROMGAZ S.A. Mediaș, Romania
[4] National University of Science and Technology Politehnica Bucuresti, Romania
e-mail (corresponding author): alexstoica97@yahoo.com; gabisimica@yahoo.com

DOI: 10.51865/JPGT.2024.02.23

ABSTRACT

Modeling the behavior of natural gas wells during exploitation is often an essential step in studying the evolution of natural gas production. However, the theoretical simulation models of wells placed on depleted deposits usually gave results different from the reality in the field. This was due to problems with the integrity of the productive strata, especially with the degree of sealing of the existing wells. The present work attempts to develop and carry out a rigorous research program of a deposit from the Sarmatian deposits of the Transylvania basin. In the paper it is presented a theoretical framework through which the behavior of the depleted field can be followed by discretizing the field and setting some discrete properties (in the case present the deposit pressure), which by expanding the modeling can serve to identify poorly drained areas, which can be exploited in the future, contributing to the increase of the final recovery factor. This discretization was achieved through the system of grid blocks, for which the average properties (temperature, pressure, permeability, etc.) and connectivity between them were modeled through the flow coefficients. The theoretical model applied to the particular deposit, which can be extended for future production provisions, by setting time intervals e.g. to a month/year instead of days and extending the grid over the entire surface of the field, not only for the central area, where the wells are grouped.

Keywords: Transylvania basin, depleted gas reservoir, well integrity, gas flow modeling, gas field modeling, gas production

INTRODUCTION

Natural gas deposits forming a complex set of pore systems and channels with different degrees of connection and varied geometry. Deposits are often considered homogeneous and uniform in modeling processes, but this is far from the reality in the most of the cases. The accentuated depletion of the gas fields highlights their heterogeneity, the irregular

shapes of the sedimentary bodies that are manifested by production anomalies. Another major impediment in gas theoretical development is the non-linearity of the flow equations due to the variation of properties with pressure. [1],[2]

Due to their general incompressibility, the motion of incompressible fluids is described by much simpler equations. For the most part, reservoir simulation methods also offer solutions for gas flow modeling, thus solving the flow problems.

Reservoir simulation has become a standard method in reservoir engineering. It is used to solve flow research problems, design horizontal wells, and simulate and analyze the increase in the final recovery factor. Along with the development of many applications, the role of these simulations has grown significantly by reducing the costs allocated to them and increasing the speed of obtaining solutions. [3],[4]

The most crucial aspect of reservoir simulation is the ability to provide realistic predictions of future gas production. As a methodology, a different number of simulation cases are generally developed, which are finally compared with each other to obtain the right decisions in the extraction process. The choice of drilling locations can be crucial in obtaining the results, the flow rates obtained, the methods of liquid injections, and the interception of the optimal positions in the reservoir because they can vary from case to case, influencing the final results. [5],[6],[7],[8]

The data for the simulation is obtained from existing information such as logs, data from mechanical cores extracted, geological descriptions, interpreted seismic data, pressure data obtained during exploitation, and production data. In most cases, a rich production history exists for depleted fields [5],[6],[7],[8]. The simulation is used to get past productions starting from the current results; thus, after comparing the results with those existing in the production history, the parameters used in the simulation can be calibrated, with the result being close to actual provisions. The model thus obtained is successfully used for future production predictions.

This paper introduces the flow approximation method using finite difference theory as an alternative to analytical solutions. This method, also called numerical simulation, has a rich specialized literature, both for mathematical elaboration and for comparing with the results obtained worldwide for different types of hydrocarbon deposits [9].

PRACTICAL ASPECTS OF NUMERICAL MODELING IN DEPLETED RESERVOIRS

Numerical modeling uses a complex mathematical description; the most elegant solutions of finite differential equations are those used in matrix or even tensor algebra (which was not presented in this paper). The benefits of sophisticated calculations are visible predominantly in the case of depleted deposits, where the need to increase the final recovery factor leads to a "desperate" search for solutions to achieve the desired goal. For adequate knowledge of the behavior of the depleted deposit, implicitly reducing the costs of some works, which may not bring the expected benefits, the numerical simulation provides a suitable framework for understanding the dynamic behavior.

Using the mentioned method, it is possible to identify the possible undrained or poorly drained areas of the deposit, the drainage limits between adjacent wells, the expansion of

the depression cone during production, interferences between wells or asymmetric flow borders, and impenetrable for productive wells. In the following, we will analyze some of the problems mentioned and indicate the calculation methods by which their solutions are reached.

MODEL CALIBRATION OF DATA IN THE EQUATION BY PRODUCTION HISTORY

A common use of reservoir simulation methods is calibrating reservoir parameters using existing production data. This process estimates reservoir properties by finding those simulation parameters with which the obtained results match the recorded production data. This procedure is also called the inverse problem because starting from the answer (reservoir performance data), we try to define the problem (reservoir description).

Reservoir performance data are usually production flow data and pressure recovery curve data. Of course, this data can contain errors, which become critical to elaborating the fit of the production data to the model predictions. For our discussion, however, this is an acceptable accuracy for the existing data.

A fundamental principle for matching production data to modeling parameters is that the solution is not unique. Multiple data sets can serve the results and match those from the production history. It becomes the responsibility of the production engineer to select the data set that is closest to reality. Other sources also use them, such as logs, production tests, mechanical core analysis, and geological interpretations.

Much work has been done on automating the fitting of measured pressure data. Still, the truth is that good results are obtained by iterative error approximation, where the engineer uses his knowledge to change parameters and iterate through the calculations until the correct result is obtained. In this process, the engineer attempts to match the historical pressure data to that obtained from the simulation.

COMPARISON OF GRID PRESSURE WITH RECOVERY CURVES

It is possible to fit the p_{df}, but in many cases, this fit is not perfect due to missing pressure data or existing errors in gas flow measurements. Fitting to data from recovery curves makes pressure much more common and believable.

The modeling problem is primarily that the test timescale needs to be longer to accurately model the grid at the reservoir level due to the size of the grid blocks. Peaceman's work provides a method for comparing grid pressures with recovery curve data [9]. The pressure profile is assumed to be a semi-steady flow.

The pressure in the block is somewhere between the p_{df}, and the average reservoir pressure. The pressure of the grid block corresponding to the data of the recovery curves and lies on a straight line on the semi-logarithmic scale at the time calculated by:

$$\Delta t_0 = \frac{67.5\phi\mu c_t \Delta x^2}{k} \quad (1)$$

If $p_0 = p_{ij}$, the block pressure, then the simulator correctly models the behavior of the reservoir.

MODEL CALIBRATION BY PRESSURE HISTORY

After finding the method for finding the correct pressure to match the production history data, we discuss how the simulator data must be modified to be consistent with the production history. This is done by the multiple trial error reduction method.

First, the reservoir sizing must match the initial gas resource. The model is considered without water influx, generally valid for gas deposits in the Transylvania basin. [6],[7]

During semi-steady flow, each point in the deposit is depleted at a rate given by the formula:

$$\frac{dp}{dt} = \frac{-qB_g}{V_p c_t} \tag{2}$$

The pressure p and the volume V_p can be represented as a summation of contour maps of Φh without being able to separate the effects of Φ and h.

The total compressibility, c_t, equals $c_f + c_g S_g + c_w S_w$. The most important term is cg, up to a pressure of 480 bar, above which the role of cf becomes paramount. The last term is generally less important than the others.

Once the initial resource value is found, the transient flow behavior must be matched after the semi-stationary behavior. The pressure drop is inversely proportional to the transmissivity, oh, and the period of the pressure drop is inversely proportional to the diffusivity, $k/(\Phi \mu c_t)$. These relationships can be observed in dimensionless pressure drop and dimensionless time in transient well flow tests.

Another method of adjusting the kh value is from the analysis of pressure profiles, the variation of pressure with distance at a particular time. If there is fluid migration (Fluid migration refers to the movement of fluids, such as liquids and gases, through a porous medium or open spaces. This phenomenon is studied in various fields, including fluid mechanics, geology, and petroleum engineering.) within the reservoir, the magnitude of the pressure gradient is inversely proportional to the kh.

Generally, the analysis by production history is much more complicated than the previous descriptions. The inhomogeneity of the deposit is highlighted in the case of drilling new wells, as the results are far below expectations. The lack of continuity of the deposit is surprising in many cases. Isolating, or partially isolating, faults complicate the situation again and are very difficult to detect. Production history analysis invokes well-by-well analysis with the multiple-trial error reduction method for these cases. The irregular 3D layout of deposits further complicates correspondence with production history.

Due to the size of the deposits, the geological phenomena that formed the basis of their formation, and the subsequent tectonic movements that affected it, the engineer can only be partially convinced of the correctness of the description of the studied deposit.

PROBLEMS RELATED TO PRODUCTION ESTIMATION

Perhaps the most important task of numerical modeling is to predict the future performance of the reservoir. When corresponding to the production history, the flows are specified for the entire period studied. These flows are unknown for future periods,

so it is necessary to specify other conditions. Thus, the most common method is to fix the pdf and calculate the flows using the simulation model for each studied time interval.

Perhaps the most important task of numerical modeling is predicting the reservoir's future performance. When corresponding to the production history, the flows are specified for the entire period studied. Since these flows are unknown for future periods, other conditions must be specified. Thus, the most common method is to fix the PDF and calculate the flows using the simulation model for each studied time interval.

The objective of numerical reservoir simulations is generally to serve alternative provisions that help make future decisions. A base case is created, from which other cases are started, depending on the results of alternative operations, such as drilling new wells, mounting field compressors, flow stimulation operations in wells, or fluid injections in wells (in the case of underground storage). Operational decisions will be made based on performance provisions closely connected with economic analyses.

FIELD DATA PROCESSING

The gas deposit modeled in this article is part of the structures created above the salt domes in the east-central part of the basin. It is a mature deposit with over 50 years of production history. The extracted gas is lean, with an exclusive methane content (99%). [1]. According to the research to be carried out, the origin of the gases is mostly thermogenic, but the existence of biogenic sources [10],11], which may be responsible for filling the deposits in a proportion of 10-15%, is not excluded either.

The main sources of gas are the marly shales of the Lower Badenian, located at a depth of over 3000 m. The migration paths to the gas traps are fault planes due to the combined effect of regional tectonics and salt movement. The deposits include shelf-margin turbidite sandstones and mid-shelf depositional systems, with some prodeltas deposits. Shielding is achieved by layers of marine clays developed between active cycles of sedimentation. [10],11],[12],[13]. The mechanism of gas displacement is their elastic expansion without significant advancements of marginal water. [6],[7].

For modeling, a complex consisting of four sandy packages, numbered Sarmatian-1, Sarmatian-2, Sarmatian-3, and Sarmatian-4, was chosen. Four wells open this complex, which is still producing today (Figure 1).

From the parallelization, it can be seen that the wells have a different degree of opening over the studied complex. The last column shows the current equipment, with the productive perforations, the isolation mirror, and the extraction pipes. The first column indicates the measured depths from sea level. Columns 2-3 show the geophysical diagraphs of PS and resistivities, and column 4 shows the gas and water zones.

The deposit areas were selected based on the electrical diagraphs, and then a 3D model was created to identify the pore volumes. Wells that traversed this complex but had no open intervals over it was also used for this model.

Figure 2 shows a vertical section through the 3D reservoir model. It shows the four wells from the experiment, with the SP diagram (right) and the deposits (red, left). Three-dimensional deposits are represented in yellow.

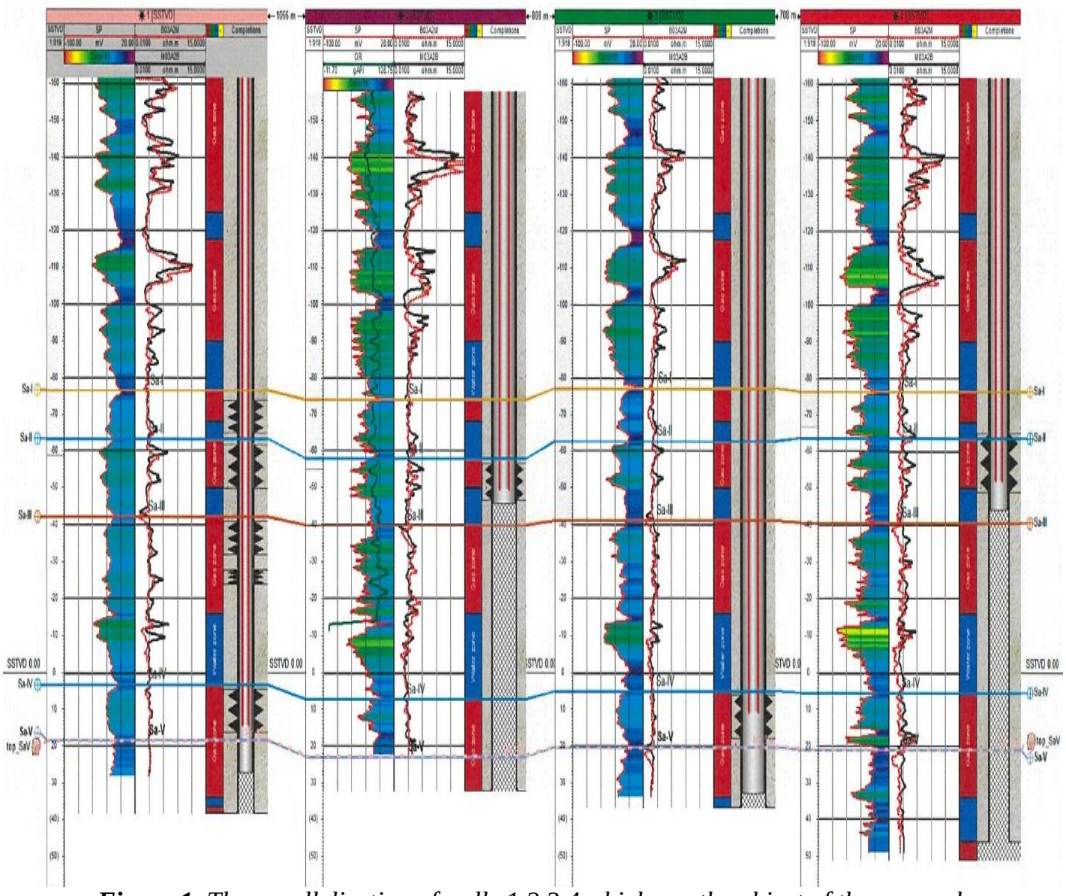

Figure 1. *The parallelization of wells 1,2,3,4 which are the object of the research*

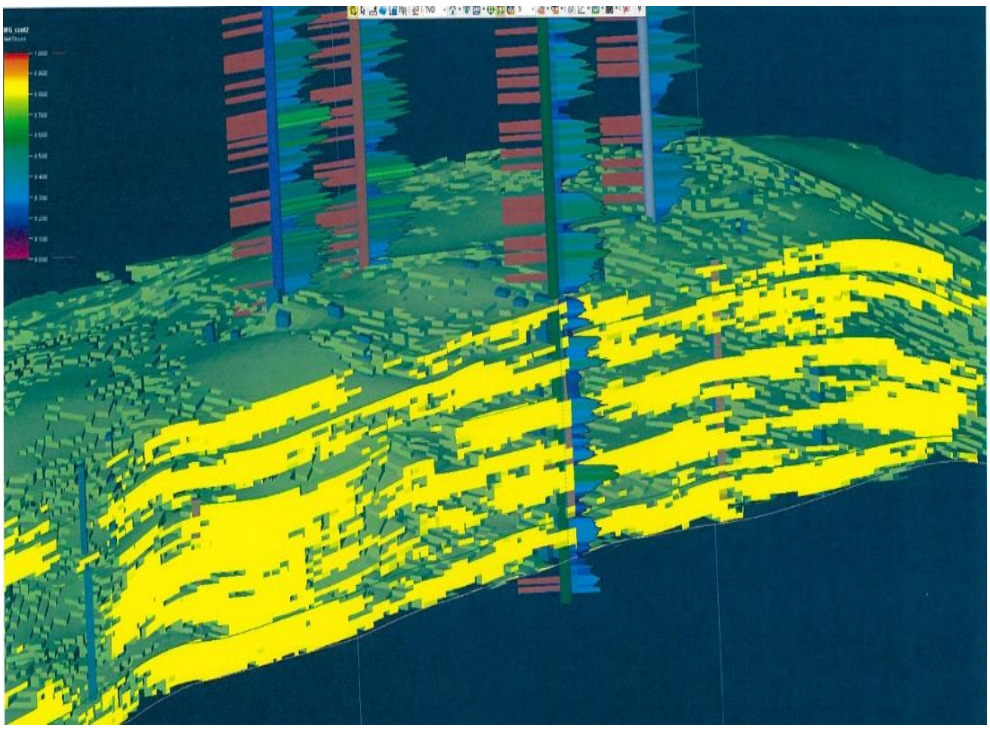

Figure 2. *Effective thickness in 3D (with yellow collectors)*

According to the 3D model, the isopach map of the complex was constructed (Figure 3). Studying the map, we notice that the maximum deposit thickness is in the central part, between 35 and 40 m.

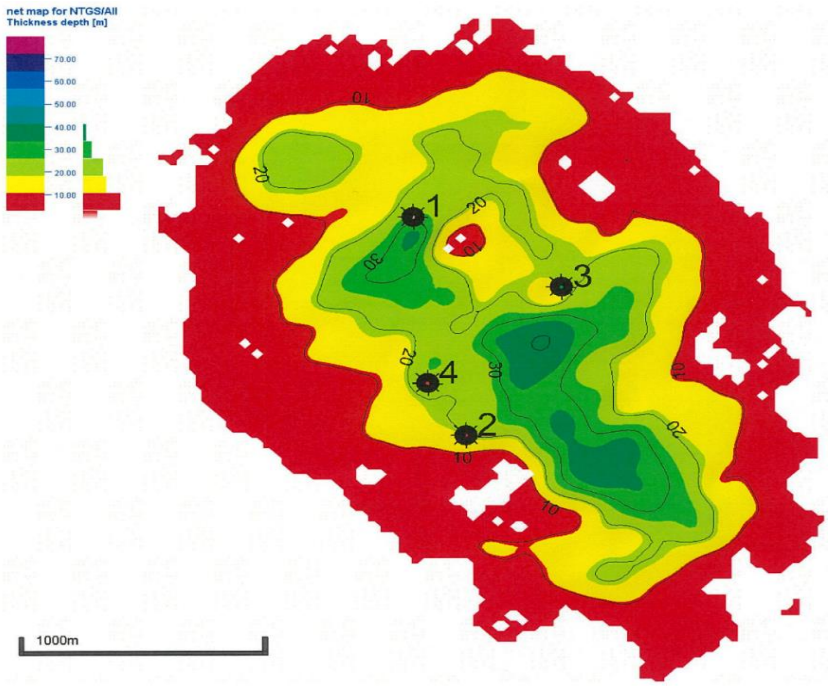

Figure 3. *Isopach map of the studied Sarmatian complex*

Without sufficient data, which can provide us with anisotropy trends and properties within the complex, we will continue to work with average values determined from the production history and measurements performed. From the analysis of the mechanical cores extracted from research wells for this complex as well as the complex petrophysical interpretations after saturation investigations in the cased hole, respectively the depth measurements carried out by PVT correlated with regional gradients, average values for physical properties of the complex:

- Complex average porosity = 30% of studies, 22-25% of cores. For the calculations, the value of 25% was considered,
- Complex average gas saturation = 70%
- Horizontal permeability = 1.5-2 mD from cores, 5-11 mD from production tests.
- Vertical permeability = 1.3-1.7 mD from cores
- Deposit temperature, for complexes = 291-294 K, 292 K average
- Initial reservoir pressure, for complexes = 35-45 bar
- Gas deviation factor, for complexes = 0.925-0.913
- Gas volume factor, for complexes = 0.027-0.021
- Depths of gas/water contacts, for complexes = +68 m ... -26 m
- Average elevations = 398.3 m.

These values are used as input data for modeling. For permeability, the average value of 7 mD was considered.

FIELD MODELING

The deposit chosen for numerical modeling was translated into Petrel software from Schlumbeger [14]. The first step in numerical modeling the complex is to choose the right grid, which provides sufficient flow stability while being small enough to observe the effects of the test. From an economic point of view, it is not advisable to close wells for research for a long period of time. [2],[7],[15].

Taking into account the aspects of the production history and results from the economic factor, the grid dimensioning was by creating blocks of 300 x 300 m in the N-S and E-W directions, the height of the cells being given by the average effective thicknesses in the block (according to the 3D model).

The 3D model of the grid block system is shown in Figure 4. Different cell colors represent their net rock volume. Wells 1,2,3,4 each intercept a separate block without being located in the same block.

Figure 5 shows the 2D map for the block system. When comparing it with Figure 6, we must remember that the differences between them are primarily due to the resolution of the grid blocks, which averaged the values inside them.

The central part of the grid block, where the said wells are also located, was selected to reduce the duration of the test and, implicitly, the economic consequences of closing the wells for a more extended period. The research period of 6-7 days ensured that, practically, the drainage limit during this period would be almost identical to the area marked in Figure 6.

The numbering of the blocks in the grid was from west to east, respectively, from north to south, totaling 3 x 5 = 15 blocks for the grid. Boundary conditions were set on the boundary of the marked rectangle around the 15 cells. The block volume calculation was done using the Petrel application (Petrel E&P Software Platform**)**, and the grid-block system was also used.

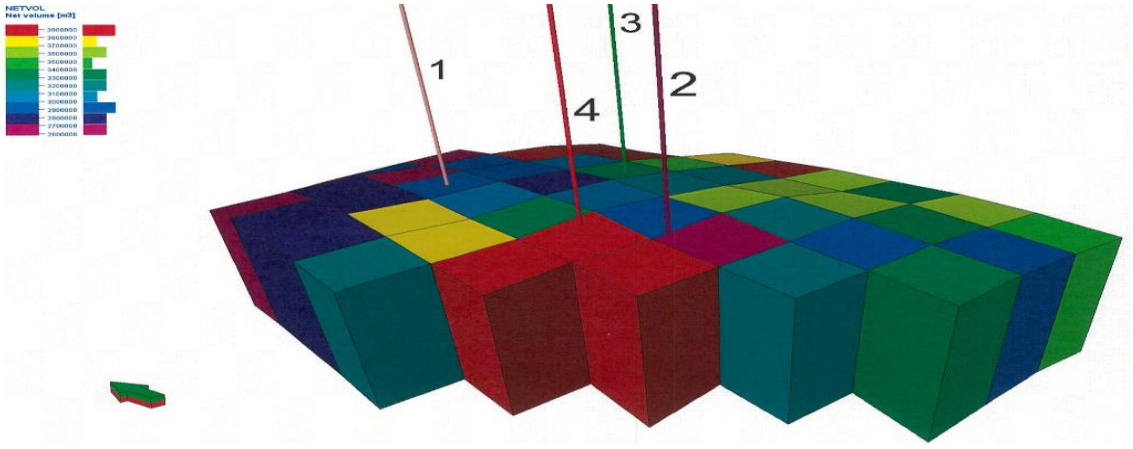

Figure 4*. Presentation of the grid block system in 3D*

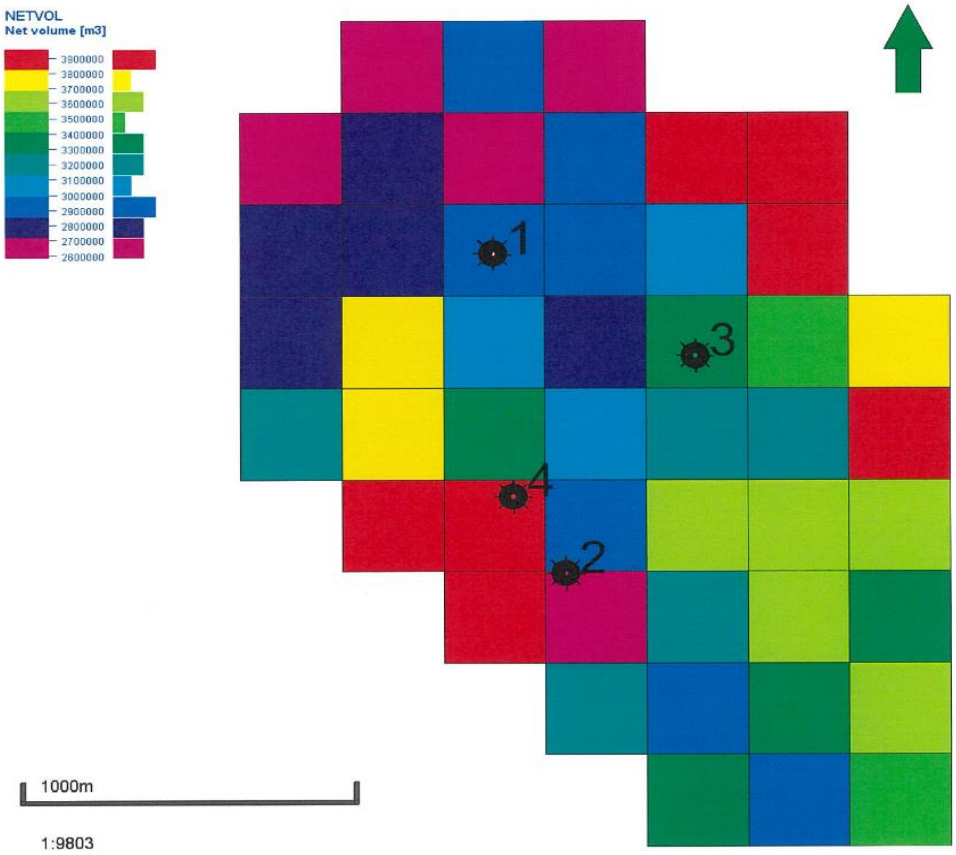

***Figure 5**. Realization of the grid block over the studied complex in 2D*

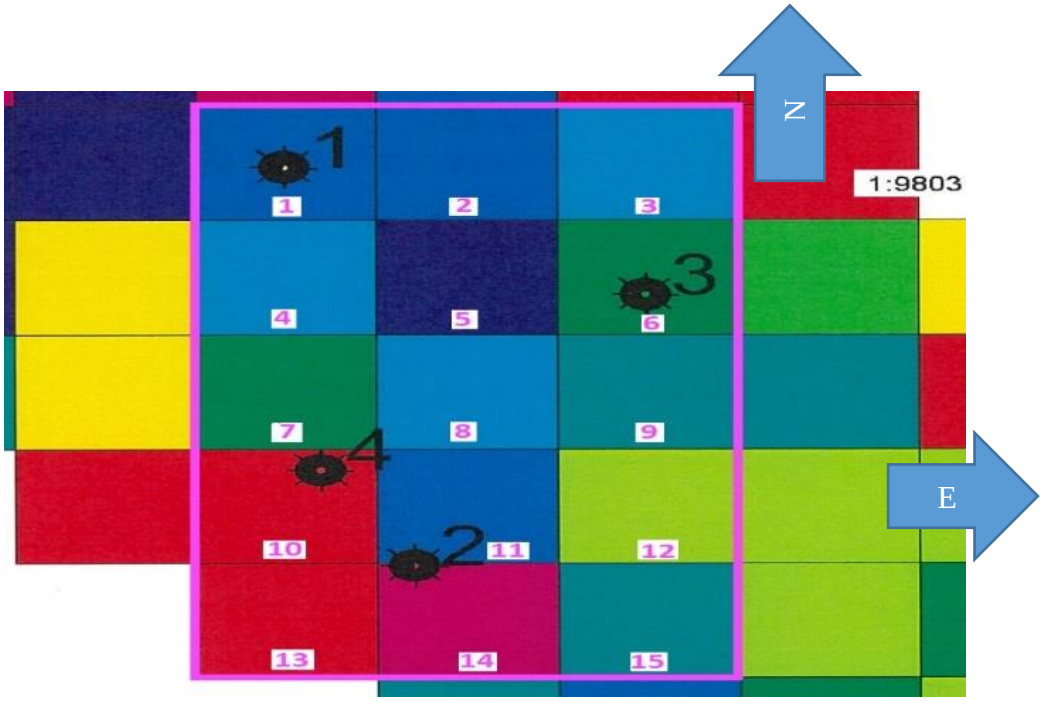

***Figure 6**. The nomenclature of the blocks in the grid that enter the numerical modeling*

Table 1. *The volume of blocks in the simulation grid*

Block	***Net Volume net, m^3***	***Porosity***	***Sg***	***Gas pore volume, m^3***	***Block height h, m***	***Well***
1	2929026	0.25	0.7	512579.55	5.70	**1**
2	2901697	0.25	0.7	337189	3.75	
3	3100742	0.25	0.7	257676	2.86	
4	3013325	0.25	0.7	420404	4.67	
5	2737781	0.25	0.7	363877	4.04	
6	3402056	0.25	0.7	302983	3.37	**3**
7	3408791	0.25	0.7	280179	3.11	
8	3121556	0.25	0.7	374340	4.16	
9	3191834	0.25	0.7	504504	5.61	
10	3885491	0.25	0.7	190635	2.12	**4**
11	2949735	0.25	0.7	320866	3.57	
12	3599647	0.25	0.7	466026	5.18	
13	3955324	0.25	0.7	89428	0.99	
14	2696601	0.25	0.7	117350	1.30	**2**
15	3219335	0.25	0.7	236341	2.63	

DESCRIPTION OF THE MODEL

The flow of natural gases will be modeled in the presented grid blocks, and the theoretical results will be verified by precision measurements in the boreholes. The records' data will validate the model data or help recalibrate some input values, ensuring closeness to the deposit's fundamental parameters. [2],[6],[7],[13]

The experiment consisted of two stages:

1) Simultaneous closing of the wells, with the introduction of bottom manometers inside, for recording the recovery curves of the static pressure,
2) Opening wells 1,2 and 3, well 4 being the control well. The wells were left in dynamic flow for 6 days, during which time the static pressure variation in well 4 was recorded.

The results were compared with results from numerical modeling. In addition to validating the model, they also verified the connectivity between the blocks to determine the areas of influence between the investigated wells.

The stages of the experiment included the following steps:

1) Pressure-temperature devices were introduced in wells 1, 2, 3, and 4, with ND measurements, having the following stations:
   - Well 1 (deposited at 335m): 0, 150 m, 250 m, 300 m, 333 m;
   - Well, 2 (deposited at 320 m, possibly annular sleeve but allowing gas flow): 0, 200 m, 250 m, 300 m, 318 m;
   - Well 3 (placed at 428 m): 0, 150 m, 300 m, 410 m, 426 m;
   - Well 4 (deposited at 297 m): 0, 100 m, 200 m, 275 m, 295 m.

2) Wells 1, 2, 3, and 4 were closed to restore static pressure (48 h), with a cumulative flow of ~ 11 thousand Sm3/day. The recorded and interpreted data served to calibrate the static pressure of the blocks of the simulation grid and correct the average permeability in each block.
3) Wells 1, 2, and 3 were opened (cumulative flow ~ 9.5 thousand Sm3/day) with well 4 closed, and the dynamic pressures at the CE in the flow were monitored for 6 days.
4) After this time, the devices were extracted from the wells, not before performing dynamic levels in wells 1, 2, and 3 and static levels in well 4 with the previously established stations to validate the single-phase flow on which the simulation is based. After extracting the device, well 4 was also opened, and the results from the bottom manometer data were interpreted.

Bottom gauge records showed the following:

1) Wells 1, 2, and 3 were clean, without liquid levels in the sole, and did not need such hydrostatic corrections for reservoir pressure.
2) Well 4 instead accumulated a water level of approximately 50 m, thus responsible for a loss of static pressure at the surface of ~ 5 bar. This accumulation is probably due to the more extended shut-in period of that well compared to the others.

MATHEMATICAL MODELING OF NATURAL GAS RESERVOIR BEHAVIOR

The grid block method will continue to be used to build the gas flow simulator, but instead of pressure, the pseudo-pressure terms of the real gas, p(p), will be used. [9], [16].

Starting from equation (3):

$$\left(\frac{\rho}{\mu}\cdot T_w\right)(p_{i-1}^{n+1}-p_i^{n+1})+\left(\frac{\rho}{\mu}\cdot T_E\right)(p_{i+1}^{n+1}-p_i^{n+1})=\left(\frac{\Delta x\Delta yh}{\Delta t}\right)[(\rho\phi_i^{n+1})-(\rho\phi_i^{n})]+ +\rho_{SC}q \quad (3)$$

Dividing the equation by ρ_{SC}, we obtain the flow form under standard conditions:

$$\left(\frac{T_{SC}}{\rho_{SC}T}\cdot\frac{\rho}{z\mu}\cdot T_w\right)(p_{i-1}^{n+1}-p_i^{n+1})+\left(\frac{T_{SC}}{\rho_{SC}T}\cdot\frac{\rho}{z\mu}\cdot T_E\right)(p_{i+1}^{n+1}- -p_i^{n+1})=\frac{1}{\Delta t}\left(\frac{T_{SC}}{\rho_{SC}T}\right)\left[\left(\frac{V_p p}{z}\right)_i^{n+1}-\left(\frac{V_p p}{z}\right)_i^{n}\right]+q \quad (4)$$

where:

$$\frac{\rho}{\rho_{SC}}=\frac{1}{B_g}=\frac{T_{SC}}{p_{SC}T}\cdot\frac{p}{z} \quad (5)$$

We now introduce the presuppression of the real gas. This has the form:

$$p_p(p)=2\int_0^p\frac{p}{z\mu}dp \quad (6)$$

We note that the value in brackets is an integrated average of the affected pressures [16].

$$\Delta p_p(p)=\left(\frac{2p}{z\mu}\right)\Delta p \quad (7)$$

Using pseudopressure notation, we can put the flow terms into more familiar forms. Let's start with the easterly flow term:

$$\left(\frac{T_{SC}}{p_{SC}T}\cdot\frac{\rho}{z\mu}\cdot T_E\right)\left(p_{i+1}^{n+1}-p_i^{n+1}\right) \quad (8)$$

We modify them slightly:

$$\left(\frac{T_{SC}}{p_{SC}T}\cdot\frac{1}{2}\cdot T_E\right)\left(\frac{2p}{z\mu}\right)\left(p_{i+1}^{n+1}-p_i^{n+1}\right) \quad (9)$$

Finally we have:

$$\left(\frac{T_{SC}}{p_{SC}T}\cdot\frac{1}{2}\cdot T_E\right)\left(p_{pi+1}^{n+1}-p_{pi}^{n+1}\right) \quad (10)$$

We simplify the term by introducing a flow coefficient, a_E:

$$a_E=\frac{T_{SC}}{p_{SC}T}\cdot\frac{1}{2}\cdot T_E \quad (11)$$

Thus the flow, expressed in Anglo-Saxon units becomes, where a_E is the easterly flow coefficient [3]:

$$a_E\left(p_{pi+1}^{n+1}-p_{pi}^{n+1}\right) \quad (12)$$

For flow from the i-1 direction, we use the westerly flow coefficient, a_W, so the equation becomes:

$$a_E\left(p_{pi+1}^{n+1}-p_{pi}^{n+1}\right)+a_W\left(p_{pi-1}^{n+1}-p_{pi}^{n+1}\right)=\frac{1}{\Delta t}\left(\frac{T_{SC}}{p_{SC}T}\right)\left[\left(\frac{V_p p}{z}\right)_i^{n+1}-\left(\frac{V_p p}{z}\right)_i^{n}\right]+q \quad (13)$$

We simplify the right side of the equation by substituting:

$$\frac{1}{\Delta t}\left(\frac{T_{SC}}{p_{SC}T}\right)\left[\left(\frac{V_p p}{z}\right)_i^{n+1}-\left(\frac{V_p p}{z}\right)_i^{n}\right]=\propto\left(p_i^{n+1}-p_i^{n}\right) \quad (14)$$

where:

$$\propto=\frac{1}{\Delta t}\left(\frac{T_{SC}}{p_{SC}T}\right)\frac{\left[\left(\frac{V_p p}{z}\right)_i^{n+1}-\left(\frac{V_p p}{z}\right)_i^{n}\right]}{\left(p_{pi}^{n+1}-p_{pi}^{n}\right)} \quad (15)$$

The flow equation for real gas is simplified as follows:

$$a_E\left(p_{pi+1}^{n+1}-p_{pi}^{n+1}\right)+a_W\left(p_{pi-1}^{n+1}-p_{pi}^{n+1}\right)=\propto\left(p_{pi}^{n+1}-p_{pi}^{n}\right)+q \quad (16)$$

The solution was made according to the Gauss-Jordan elimination method. This algorithm solves systems of linear equations and compu0tes the inverse of a nonsingular matrix. This transforms the matrix into a reduced row echelon form, simplifying solving the equations.

NUMERICAL MODELING FOR FLOW IN FIELD ANALYSIS

Due to some uncertainties of the 3D model (geometry modeled for the adequate thickness between the wells), the approximation values when solving the equations (9 digital from Excel), the transformations of pressure to pseudo pressure and vice versa, the final pressure values were slightly modified from the constant value of 15.10 bar.

Studying the graph, we can see a progressive download of the blocks. The most apparent pressure drops are for blocks 1, 6, and 14, which have harmful sources (wells with

production). The drop at block 15 is probably due to the need for a finer grid system that eliminates the interference between blocks 14 and 15.

It is also interesting to note the interconnectivity of blocks 5, 8, and 11 with the neighborhoods. Their high values between productive blocks indicate that their connectivity with neighboring blocks is not optimal.

In the following, we will use the Anglo-Saxon units of measurement to ensure consistency in the calculations. This is necessary because the tables and graphs for calculating the real gas pseudo-pressure are expressed like this. Thus, volumes are expressed in cf (cubic feet), pressure in psi (psi), permeability in md (military), and temperature in gr. Rankine, etc.

Starting from the presented geometry of the blocks, we have the volume transformation (Table 2). Each block in the grid has blocks in the neighborhood of the north (n), east (e), south (s) and west (w) blocks, less the side cells, where the lack of a neighboring block is marked with 0. The own block is marked centrally (c). Using this convention we have the nomenclature of the simulation grid as follows: neighboring cells and calculation cells. According to this table, for example cell 9 has neighbors cells 6 (N), 8 (W), 0 (none in E) and 12 (S).

***Table 2**. The volume of the blocks prepared for the modeling calculation*

Vp, m3			**Vp, ft3**			**Vpg, ft^3 modify whith P, Sg**		
2929026	2901697	3100742	103437674	102472559	109501774	18101593	17932698	19162810
3013325	2737781	3402056	106414668	96683915	120142587	18622567	16919685	21024953
3408791	3121556	3191834	120380432	110236814	112718660	21066576	19291442	19725766
3885491	2949735	3599647	137214949	104169007	127120454	24012616	18229576	22246079
3955324	2696601	3219335	139681080	95229655	113689850	24444189	16665190	19895724

This order is also used in the modeling matrix calculus. Using the established reference values (1) (k =7 mD, T_{sc} =518.4 ^{o}R, p_{sc} =14.7 psia, T_r =525.6 ^{o}R, dx =dy =300 m), using formulas 3-16, we have the flow coefficients in directions T_{NESW}, a_{NESW} (Table 3). These coefficients are constant throughout the modeling, depending only on the geometry of the blocks and constant physical values.

The reservoir pressures were measured for the experiment, with the values: well 1=15.10 bar, well 2=12.40 bar, well 3=17.80 bar, and well 4=13.80 bar. These pressures were assigned to cells 1, 6, 10, and 14, as initial pressures. The values are different because they have various degrees of depletion.

The initial static values were extrapolated between them as input values to the modeling. The values were transformed into real gas pseudo pressures [4] (Table 4). The calculation of the initial deviation factor Z for real gases was calculated according to the Dranchuk and Abou-Kassem corelation, [4], the gas being considered pure methane, (Table 4).

Table 3.a,b,c. *Flow coefficients for modeling*

	1	2	3	4	5	6	7	8	9	10	11	12	13	14	15
1	C	E	0	S	0	0	0	0	0	0	0	0	0	0	0
2	W	C	E	0	S	0	0	0	0	0	0	0	0	0	0
3	0	W	C	0	0	S	0	0	0	0	0	0	0	0	0
4	N	0	0	C	E	0	S	0	0	0	0	0	0	0	0
5	0	N	0	W	C	E	0	S	0	0	0	0	0	0	0
6	0	0	N	0	W	C	0	0	S	0	0	0	0	0	0
7	0	0	0	N	0	0	C	E	0	S	0	0	0	0	0
8	0	0	0	0	N	0	W	C	E	0	S	0	0	0	0
9	0	0	0	0	0	N	0	W	C	0	0	S	0	0	0
10	0	0	0	0	0	0	N	0	0	C	E	0	S	0	0
11	0	0	0	0	0	0	0	N	0	W	C	E	0	S	0
12	0	0	0	0	0	0	0	0	N	0	W	C	0	0	S
13	0	0	0	0	0	0	0	0	0	N	0	0	C	E	0
14	0	0	0	0	0	0	0	0	0	0	N	0	W	C	E
15	0	0	0	0	0	0	0	0	0	0	0	N	0	W	C

cells to calculation

neighboring cells

a

blocks	Vp, m3	Vpg, cf	h, m	h, ft	h_w, ft	h_N, ft	h_E, ft	h_S, ft	T_w	T_N	T_E	T_S
1	512579.55	18145316	5.7	19	0	0	106	110	0.0000	0.0000	4.6870	4.8673
2	507796.98	17976013	5.6	19	107	0	113	100	4.7312	0.0000	5.0085	4.4222
3	542629.85	19209097	6.0	20	106	0	0	124	4.6870	0.0000	0.0000	5.4952
4	527331.88	18667548	5.9	19	0	107	100	124	0.0000	4.7312	4.4222	5.5061
5	479111.68	16960553	5.3	17	110	106	124	114	4.8673	4.6870	5.4952	5.0421
6	595359.8	21075737	6.6	22	100	113	0	116	4.4222	5.0085	0.0000	5.1557
7	596538.43	21117460	6.6	22	0	110	114	142	0.0000	4.8673	5.0421	6.2761
8	546272.3	19338039	6.1	20	124	100	116	108	5.5061	4.4222	5.1557	4.7646
9	558570.95	19773412	6.2	20	114	124	0	131	5.0421	5.4952	0.0000	5.8144
10	679960.93	24070617	7.6	25	0	124	108	144	0.0000	5.5061	4.7646	6.3889
11	516203.63	18273608	5.7	19	142	114	131	98	6.2761	5.0421	5.8144	4.3557
12	629938.23	22299813	7.0	23	108	116	0	117	4.7646	5.1557	0.0000	5.2001
13	692181.7	24503232	7.7	25	0	142	98	0	0.0000	6.2761	4.3557	0.0000
14	471905.18	16705443	5.2	17	144	108	117	0	6.3889	4.7646	5.2001	0.0000
15	563383.63	19943780	6.3	21	98	131	0	0	4.3557	5.8144	0.0000	0.0000

b

a_w	a_N	a_E	a_S	Sum
0.00000	0.00000	0.15724	0.16329	0.32053
0.15872	0.00000	0.16802	0.14836	0.47510
0.15724	0.00000	0.00000	0.18435	0.34159
0.00000	0.15872	0.14836	0.18472	0.49179
0.16329	0.15724	0.18435	0.16915	0.67403
0.14836	0.16802	0.00000	0.17296	0.48934
0.00000	0.16329	0.16915	0.21055	0.54299
0.18472	0.14836	0.17296	0.15984	0.66588
0.16915	0.18435	0.00000	0.19506	0.54856
0.00000	0.18472	0.15984	0.21433	0.55889
0.21055	0.16915	0.19506	0.14612	0.72088
0.15984	0.17296	0.00000	0.17445	0.50725
0.00000	0.21055	0.14612	0.00000	0.35667
0.21433	0.15984	0.17445	0.00000	0.54863
0.14612	0.19506	0.00000	0.00000	0.34118

c

Table 4. *The initial pressures and pseudo-pressures of the blocks in the grid (to the wells analysis 1,2,3)*

Initial pressures, bar		
15.1	15.1	15.1
15.1	15.1	15.1
15.1	15.1	15.1
15.1	15.1	15.1
15.1	15.1	15.1

initial pressures, psia		
234	234	234
234	234	234
234	234	234
234	234	234
234	234	234

initial pp, psia2/cp		
3786774	3786775	3786775
3786775	3786775	3786774
3786775	3786775	3786775
3786775	3786775	3786775
3786775	3786774	3786775

Table 5. *Initial Z values, used for modeling to the wells analysis 1,2,3*

0.968	0.968	0.968
0.968	0.968	0.968
0.968	0.968	0.968
0.968	0.968	0.968
0.968	0.968	0.968

The next coefficients to calculate are α, a_c and d. Applying the limit difference, for the delta(p/z)/delta(p_p) value, the variations at the beginning having very small values, it can be approximated for each cell, the value equal to 1.

The flow rates in the experiment, expressed in SCFD, were 148486 for well 1, 63629 for well 2 and 116653 for well 3. The q values in the grid, considered constant throughout the experiment, are those in Table 6. The calculated initial values for are α, a_c and d are shown in Tables 7, 8 and 9.

Table 6. *The starting flow rates to the wells analysis 1,2,3 (q is measurenment in scfD)*

148468	0	0
0	0	116653
0	0	0
0	0	0
0	63629	0

Table 7. *The initial values α (to the wells analysis 1,2,3)*

106271.6	105280	112501.8
109330.1	99332.79	123434.2
123678.5	113257	115806.8
140974.3	107023	130603.2
143508	97838.69	116804.6

Table 8. *The initial values of the coefficient in the main diagonal of the calculation matrix (a_c)*

106271.9	105280.3	112502.1
109330.5	99333.11	123434.5
123678.8	113257.3	115807.2
140974.6	107023.3	130603.5
143508.3	97839.01	116805

Table 9. *The initial values of the vector of the calculation matrix (d)*

402426405853	398671751426	426019065347
414008614740	376150902831	467417268405
468342724349	428878755327	438534433830
533837785999	405271818075	494564930110
543432324787	370493011136	442312868255

The data presented above are those that enter the first time interval, $t = n = 1$, in the calculation process of solving the matrix equation (17) through the iteration process. The time interval, $n = 2, 3, ..., 6$, equals days (t measured in days). To obtain the solutions for the system of linear equations 15 x 15 from (17), we used the Gauss-Jordan elimination method [3],[4].

$$\begin{pmatrix}
a_c & -a_E & & -a_S & & & & & & & & & & & \\
-a_W & a_c & -a_E & & -a_S & & & & & & & & & & \\
 & -a_W & a_c & & & -a_S & & & & & & & & & \\
-a_N & & & a_c & -a_E & & -a_S & & & & & & & & \\
 & -a_N & & -a_W & a_c & -a_E & & -a_S & & & & & & & \\
 & & -a_N & & -a_W & a_c & & & -a_S & & & & & & \\
 & & & -a_N & & & a_c & -a_E & & -a_S & & & & & \\
 & & & & -a_N & & -a_W & a_c & -a_E & & -a_S & & & & \\
 & & & & & -a_N & & -a_W & a_c & & & -a_S & & & \\
 & & & & & & -a_N & & & a_c & -a_E & & -a_S & & \\
 & & & & & & & -a_N & & -a_W & a_c & -a_E & & -a_S & \\
 & & & & & & & & -a_N & & -a_W & a_c & & & -a_S \\
 & & & & & & & & & -a_N & & & a_c & -a_E & \\
 & & & & & & & & & & -a_N & & -a_W & a_c & -a_E \\
 & & & & & & & & & & & -a_N & & -a_W & a_c
\end{pmatrix}
\begin{pmatrix} p_{p1} \\ p_{p2} \\ p_{p3} \\ p_{p4} \\ p_{p5} \\ p_{p6} \\ p_{p7} \\ p_{p8} \\ p_{p9} \\ p_{p10} \\ p_{p11} \\ p_{p12} \\ p_{p13} \\ p_{p14} \\ p_{p15} \end{pmatrix}
=
\begin{pmatrix} d_1 \\ d_2 \\ d_3 \\ d_4 \\ d_5 \\ d_6 \\ d_7 \\ d_8 \\ d_9 \\ d_{10} \\ d_{11} \\ d_{12} \\ d_{13} \\ d_{14} \\ d_{15} \end{pmatrix} \quad (17)$$

Since a successive iteration of solving the system was needed due to the application of time and iteration indices, an Excel application was built for the solution, which was used to obtain the results.

The method consisted of reducing the main matrix to values of 1 for the central diagonal and 0 for the rest of the elements, finally obtaining the solution of the equation in the column of free terms.

The system's coherence was verified by a simulation with equal static starting pressures for each block, 15.10 bar, with no flow in the wells, $q = 0$ for each. We have the solution system in Table 10.

The solution was made according to the Gauss-Jordan elimination method. This algorithm is used to solve systems of linear equations and compute the inverse of a nonsingular matrix. It transforms the matrix into reduced row echelon form, which greatly simplifies solving the equations.

Table 10. *Verification matrix for Ps = 15.10 bar, q = 0*

	1	2	3	4	5	6	7	8	9	10	11	12	13	14	15	term. lib.
1	212543.5	-0.15724	0	-0.16329	0	0	0	0	0	0	0	0	0	0	0	804853108642
2	-0.15872	210560.4	-0.16802	0	-0.14836	0	0	0	0	0	0	0	0	0	0	797343502852
3	0	-0.15724	225004	0	0	-0.18435	0	0	0	0	0	0	0	0	0	852038130694
4	-0.15872	0	0	218660.6	-0.14836	0	-0.18472	0	0	0	0	0	0	0	0	828017229481
5	0	-0.15724	0	-0.16329	198665.9	-0.18435	0	-0.16915223	0	0	0	0	0	0	0	752301805662
6	0	0	-0.16802	0	-0.14836	246868.7	0	0	-0.17296	0	0	0	0	0	0	934834770116
7	0	0	0	-0.16329	0	0	247357.4	-0.16915223	0	-0.21055	0	0	0	0	0	936685448698
8	0	0	0	0	-0.14836	0	-0.18472	226514.3212	-0.17296	0	-0.15984	0	0	0	0	857757510653
9	0	0	0	0	0	-0.18435	0	-0.16915223	231614	0	0	-0.19506	0	0	0	877068867660
10	0	0	0	0	0	0	-0.18472	0	0	281948.8	-0.15984	0	-0.21433	0	0	1067675571999
11	0	0	0	0	0	0	0	-0.16915223	0	-0.21055	214046.2	-0.19506	0	-0.14612	0	810543636150
12	0	0	0	0	0	0	0	0	-0.17296	0	-0.15984	261206.7	0	0	-0.17445	989129860221
13	0	0	0	0	0	0	0	0	0	-0.21055	0	0	287016.2	-0.14612	0	1086864649575
14	0	0	0	0	0	0	0	0	0	0	-0.15984	0	-0.21433	195677.7	-0.17445	740986149531
15	0	0	0	0	0	0	0	0	0	0	0	-0.19506	0	-0.14612	233609.6	884625736511

Due to some uncertainties of the 3D model (geometry modeled for the adequate thickness between the wells), the approximation values when solving the equations (9 digital from Excel), the transformations of pressure to pseudo pressure and vice versa, the final pressure values were slightly modified from the constant value of 15.10 bar. For calibration, the correction system in Table 11 was used. These correction values will be applied to subsequent calculations for each block.

Table 11. *Final pressure calibration coefficients for each individual block*

1	0.981514536
2	0.981514066
3	0.981514476
4	0.981514035
5	0.981513397
6	0.981514098
7	0.981513960
8	0.981513560
9	0.981513906
10	0.981513995
11	0.981513339
12	0.981514079
13	0.981514456
14	0.981513790
15	0.981514448

This solution constitutes the values at the first time step, one day after opening the wells, or for n=1 in the sequence. The values are from Tables 3, 8, and 9 this time.

Analyzing the results, we notice that the values are grouped, and in this case, the application of an iteration procedure for values k=2,3,... is not justified. Using the obtained pressure values, we will proceed to the next time step, n = 2 of the modeling. It should be noted that the solutions of the matrix equation at each step are expressed in pseudo-pressure values, which are converted back into pressure described in the bar.

The correct solution of the equation, after applying the calibration to the wells, is presented in Table 12.

Table 12. *Correct solution of the equation, after applying the calibration to the wells*

15.100000000	15.100000000	15.100000000
15.100000000	15.100000000	15.100000000
15.100000000	15.100000000	15.100000000
15.100000000	15.100000000	15.100000000
15.100000000	15.100000000	15.100000000

Applying now the flow of the system, according to Table 4, the resulting matrix is presented in Table 13. Most of the values do not change, they are according to the characteristic numbers in the table. Instead, the pressure drops for blocks 1, 6 and 14 can already be seen in the results in Table 14.

Table 13. *Verification matrix for Ps = 15.10 bar, q values from table 6*

	1	2	3	4	5	6	7	8	9	10	11	12	13	14	15	term. lib.
1	212543.5	-0.15724	0	-0.16329	0	0	0	0	0	0	0	0	0	0	0	804852960174
2	-0.15872	210560.4	-0.16802	0	-0.14836	0	0	0	0	0	0	0	0	0	0	797343502852
3	0	-0.15724	225004	0	0	-0.18435	0	0	0	0	0	0	0	0	0	852038130694
4	-0.15872	0	0	218660.6	-0.14836	0	-0.18472	0	0	0	0	0	0	0	0	828017229481
5	0	-0.15724	0	-0.16329	198665.9	-0.18435	0	-0.16915223	0	0	0	0	0	0	0	752301805662
6	0	0	-0.16802	0	-0.14836	246868.7	0	0	-0.17296	0	0	0	0	0	0	934834653462
7	0	0	0	-0.16329	0	0	247357.4	-0.16915223	0	-0.21055	0	0	0	0	0	936685448698
8	0	0	0	0	-0.14836	0	-0.18472	226514.3212	-0.17296	0	-0.15984	0	0	0	0	857757510653
9	0	0	0	0	0	-0.18435	0	-0.16915223	231614	0	0	-0.19506	0	0	0	877068867660
10	0	0	0	0	0	0	-0.18472	0	0	281948.8	-0.15984	0	-0.21433	0	0	1067675571999
11	0	0	0	0	0	0	0	-0.16915223	0	-0.21055	214046.2	-0.19506	0	-0.14612	0	810543636150
12	0	0	0	0	0	0	0	0	-0.17296	0	-0.15984	261206.7	0	0	-0.17445	989129860221
13	0	0	0	0	0	0	0	0	0	-0.21055	0	0	287016.2	-0.14612	0	1086864649575
14	0	0	0	0	0	0	0	0	0	0	-0.15984	0	-0.21433	195677.7	-0.17445	740986085902
15	0	0	0	0	0	0	0	0	0	0	0	-0.19506	0	-0.14612	233609.6	884625736511

Table 14. *Pressure results to the well blocks (day one)*

15.099998183	15.100000000	15.100000000
15.100000000	15.100000000	15.099998771
15.100000000	15.100000000	15.100000000
15.100000000	15.100000000	15.100000000
15.100000000	15.099999154	15.100000000

Table 15 shows us the matrix of the system of equations for this case. The daily flows of wells 1, 2 and 3 remained identical to the first stage (n = 1).

The solutions of the system, expressed in bar, are the ones below, with the mention that once again a normalization of the values was carried out, at the maximum value from the solutions assigning 15.10 bar, thus resulting in a calibration coefficient P_{cb2} equal to 1.00000122014, with which -shared the final solutions. Thus we have the data given in Table 16.

Table 15. *The matrix of the system of equations for n =2 (the second day of the experiment)*

	1	2	3	4	5	6	7	8	9	10	11	12	13	14	15	term. lib.
1	106271.9	-0.15724	0	-0.16329	0	0	0	0	0	0	0	0	0	0	0	402426294669
2	-0.15872	105280.3	-0.16802	0	-0.14836	0	0	0	0	0	0	0	0	0	0	398671751426
3	0	-0.15724	112502.1	0	0	-0.18435	0	0	0	0	0	0	0	0	0	426019065347
4	-0.15872	0	0	109330.5	-0.14836	0	-0.18472	0	0	0	0	0	0	0	0	414008614740
5	0	-0.15724	0	-0.16329	99333.11	-0.18435	0	-0.16915223	0	0	0	0	0	0	0	376150902831
6	0	0	-0.16802	0	-0.14836	123434.5	0	0	-0.17296	0	0	0	0	0	0	467417181046
7	0	0	0	-0.16329	0	0	123678.8	-0.16915223	0	-0.21055	0	0	0	0	0	468342724349
8	0	0	0	0	-0.14836	0	-0.18472	113257.3209	-0.17296	0	-0.15984	0	0	0	0	428878755327
9	0	0	0	0	0	-0.18435	0	-0.16915223	115807.2	0	0	-0.19506	0	0	0	438534433830
10	0	0	0	0	0	0	-0.18472	0	0	140974.6	-0.15984	0	-0.21433	0	0	533837785999
11	0	0	0	0	0	0	0	-0.16915223	0	-0.21055	107023.3	-0.19506	0	-0.14612	0	405271818075
12	0	0	0	0	0	0	0	0	-0.17296	0	-0.15984	130603.5	0	0	-0.17445	494564930110
13	0	0	0	0	0	0	0	0	0	-0.21055	0	0	143508.3	-0.14612	0	543432324787
14	0	0	0	0	0	0	0	0	0	0	-0.15984	0	-0.21433	97839.01	-0.17445	370492963486
15	0	0	0	0	0	0	0	0	0	0	0	-0.19506	0	-0.14612	116805	442312868255

Table 16. *Test pressure in a two day of experiments*

15.099975221	15.099988807	15.099982498
15.099989291	15.099999103	15.099984013
15.099990435	15.099996594	15.099991274
15.099989904	15.100000000	15.099988618
15.099982817	15.099990100	15.099982447

The values being grouped, the iteration calculation was not applied this time either. These pressures were the input data for stage n = 3 (the third day of the experiment). Table 17 includes the system matrix. The solutions of the system, retransformed from psuedopressures into pressures [bar], the applied normalization coefficient being P_{cb3} equal to 1.00000244026, are presented in Table 18.

Even at these values, it is not the case to apply the iteration procedure. They serve as input data for stage n = 4, day four. Using the resulting flow coefficients, we have the matrix of the linear system (Table 19).

Table 17. *The matrix of the system of equations for n =3 (the third day of the experiment)*

	1	2	3	4	5	6	7	8	9	10	11	12	13	14	15	term. lib.
1	70848.04	-0.15724	0	-0.16329	0	0	0	0	0	0	0	0	0	0	0	268283210237
2	-0.15872	70187	-0.16802	0	-0.14836	0	0	0	0	0	0	0	0	0	0	265780715277
3	0	-0.15724	75001.54	0	0	-0.18435	0	0	0	0	0	0	0	0	0	284011954412
4	-0.15872	0	0	72887.08	-0.14836	0	-0.18472	0	0	0	0	0	0	0	0	276005293735
5	0	-0.15724	0	-0.16329	66222.18	-0.18435	0	-0.16915223	0	0	0	0	0	0	0	250767234360
6	0	0	-0.16802	0	-0.14836	82289.76	0	0	-0.17296	0	0	0	0	0	0	311610715874
7	0	0	0	-0.16329	0	0	82452.67	-0.16915223	0	-0.21055	0	0	0	0	0	312228028788
8	0	0	0	0	-0.14836	0	-0.18472	75504.98743	-0.17296	0	-0.15984	0	0	0	0	285919022133
9	0	0	0	0	0	-0.18435	0	-0.16915223	77204.88	0	0	-0.19506	0	0	0	292355901319
10	0	0	0	0	0	0	-0.18472	0	0	93983.16	-0.15984	0	-0.21433	0	0	355891310966
11	0	0	0	0	0	0	0	-0.16915223	0	-0.21055	71348.96	-0.19506	0	-0.14612	0	270181212050
12	0	0	0	0	0	0	0	0	-0.17296	0	-0.15984	87069.12	0	0	-0.17445	329709382762
13	0	0	0	0	0	0	0	0	0	-0.21055	0	0	95672.29	-0.14612	0	362287269937
14	0	0	0	0	0	0	0	0	0	0	-0.15984	0	-0.21433	65226.11	-0.17445	246994947726
15	0	0	0	0	0	0	0	0	0	0	0	-0.19506	0	-0.14612	77870.08	294874458485

Table 18. *Test pressure in a three day of experiments*

15.099920588	15.099960850	15.099938783
15.099962543	15.099996863	15.099948991
15.099966544	15.099988086	15.099969479
15.099964685	15.100000000	15.099960187
15.099939897	15.099968751	15.099938604

Table 19. *The matrix of the system of equations for n =4 (the fourth day of the experiment)*

	1	2	3	4	5	6	7	8	9	10	11	12	13	14	15	term. lib.
1	53136.11	-0.15724	0	-0.16329	0	0	0	0	0	0	0	0	0	0	0	201210699067
2	-0.15872	52640.33	-0.16802	0	-0.14836	0	0	0	0	0	0	0	0	0	0	199334689088
3	0	-0.15724	56251.23	0	0	-0.18435	0	0	0	0	0	0	0	0	0	213007549933
4	-0.15872	0	0	54665.39	-0.14836	0	-0.18472	0	0	0	0	0	0	0	0	207003128395
5	0	-0.15724	0	-0.16329	49666.72	-0.18435	0	-0.16915223	0	0	0	0	0	0	0	188075361713
6	0	0	-0.16802	0	-0.14836	61717.4	0	0	-0.17296	0	0	0	0	0	0	233706763217
7	0	0	0	-0.16329	0	0	61839.58	-0.16915223	0	-0.21055	0	0	0	0	0	234170170906
8	0	0	0	0	-0.14836	0	-0.18472	56628.8207	-0.17296	0	-0.15984	0	0	0	0	214438989196
9	0	0	0	0	0	-0.18435	0	-0.16915223	57903.74	0	0	-0.19506	0	0	0	219266199334
10	0	0	0	0	0	0	-0.18472	0	0	70487.45	-0.15984	0	-0.21433	0	0	266917459718
11	0	0	0	0	0	0	0	-0.16915223	0	-0.21055	53511.8	-0.19506	0	-0.14612	0	202635909038
12	0	0	0	0	0	0	0	0	-0.17296	0	-0.15984	65301.92	0	0	-0.17445	247280968085
13	0	0	0	0	0	0	0	0	0	-0.21055	0	0	71754.3	-0.14612	0	271713679211
14	0	0	0	0	0	0	0	0	0	0	-0.15984	0	-0.21433	48919.66	-0.17445	185245593544
15	0	0	0	0	0	0	0	0	0	0	0	-0.19506	0	-0.14612	58402.64	221154369544

The solutions of the system, retransformed from psuedopressures into pressures [bar], with the normalization coefficient applied by P_{cb4} equal to 1.00000366036, are given in Table 20.

Table 20. *Test pressure in a four day of experiments*

15.099818521	15.099907785	15.099855808
15.099911773	15.099992612	15.099883621
15.099921196	15.099971938	15.099928110
15.099916819	15.100000000	15.099906224
15.099858431	15.099928988	15.099855387

We do not apply normalization to these obtained solutions either, since they are consistent values. They enter as block pressures for stage n = 5, the fifth day of the experiment.The system matrix for this case is the one in Table 21.

The solutions of the system, retransformed from pseudopressures into pressures [bar], with the normalization coefficient applied by P_{cb5} equal to 1.00002474846, are given in Table 22.

Table 21. *The matrix of the system of equations for n =5 (the fifth day of the experiment)*

	1	2	3	4	5	6	7	8	9	10	11	12	13	14	15	term. lib.
1	42508.95	-0.15724	0	-0.16329	0	0	0	0	0	0	0	0	0	0	0	160966031380
2	-0.15872	42112.33	-0.16802	0	-0.14836	0	0	0	0	0	0	0	0	0	0	159466464568
3	0	-0.15724	45001.05	0	0	-0.18435	0	0	0	0	0	0	0	0	0	170403889986
4	-0.15872	0	0	43732.38	-0.14836	0	-0.18472	0	0	0	0	0	0	0	0	165601224295
5	0	-0.15724	0	-0.16329	39733.44	-0.18435	0	-0.16915223	0	0	0	0	0	0	0	150460192109
6	0	0	-0.16802	0	-0.14836	49373.99	0	0	-0.17296	0	0	0	0	0	0	186963528846
7	0	0	0	-0.16329	0	0	49471.73	-0.16915223	0	-0.21055	0	0	0	0	0	187334844993
8	0	0	0	0	-0.14836	0	-0.18472	45303.12067	-0.17296	0	-0.15984	0	0	0	0	171550770134
9	0	0	0	0	0	-0.18435	0	-0.16915223	46323.06	0	0	-0.19506	0	0	0	175411856066
10	0	0	0	0	0	0	-0.18472	0	0	56390.03	-0.15984	0	-0.21433	0	0	213532413622
11	0	0	0	0	0	0	0	-0.16915223	0	-0.21055	42809.5	-0.19506	0	-0.14612	0	162108727230
12	0	0	0	0	0	0	0	0	-0.17296	0	-0.15984	52241.6	0	0	-0.17445	197823151258
13	0	0	0	0	0	0	0	0	0	-0.21055	0	0	57403.5	-0.14612	0	217368250753
14	0	0	0	0	0	0	0	0	0	0	-0.15984	0	-0.21433	39135.8	-0.17445	148195566103
15	0	0	0	0	0	0	0	0	0	0	0	-0.19506	0	-0.14612	46722.18	176921256928

Table 22. *Test pressure in a five day of experiments*

15.099345417	15.099517118	15.099414036
15.099525028	15.099685348	15.099472801
15.099543716	15.099644348	15.099557428
15.099535035	15.099700000	15.099514023
15.099419239	15.099561649	15.099413202

These pressure solutions serve as input data for the last stage, n = 6, the sixth day of the experiment, with the calculation matrix of the system of equations shown in Table 23.

The solutions of the system, retransformed from pseudo pressures into pressures expressed in bar, after applying the normalization factor P_{cb6} equal to 0.99999621079, are the ones below, with yellow marking the values from the productive blocks, with violet the block with the control wells, in which the recording device followed the variation pressure during the experiment, without the need to apply iteration steps in this case as well (Table 24).

Table 23. *The matrix of the system of equations for n = 6 (the last day of the experiment)*

	1	2	3	4	5	6	7	8	9	10	11	12	13	14	15	term. lib.
1	35424.18	-0.15724	0	-0.16329	0	0	0	0	0	0	0	0	0	0	0	134128685213
2	-0.15872	35093.66	-0.16802	0	-0.14836	0	0	0	0	0	0	0	0	0	0	132880826628
3	0	-0.15724	37500.93	0	0	-0.18435	0	0	0	0	0	0	0	0	0	141993702910
4	-0.15872	0	0	36443.7	-0.14836	0	-0.18472	0	0	0	0	0	0	0	0	137992905012
5	0	-0.15724	0	-0.16329	33111.25	-0.18435	0	-0.16915223	0	0	0	0	0	0	0	125377635488
6	0	0	-0.16802	0	-0.14836	41145.04	0	0	-0.17296	0	0	0	0	0	0	155793188824
7	0	0	0	-0.16329	0	0	41226.5	-0.16915223	0	-0.21055	0	0	0	0	0	156103410471
8	0	0	0	0	-0.14836	0	-0.18472	37752.65398	-0.17296	0	-0.15984	0	0	0	0	142951854219
9	0	0	0	0	0	-0.18435	0	-0.16915223	38602.6	0	0	-0.19506	0	0	0	146168307746
10	0	0	0	0	0	0	-0.18472	0	0	46991.74	-0.15984	0	-0.21433	0	0	177933348166
11	0	0	0	0	0	0	0	-0.16915223	0	-0.21055	35674.64	-0.19506	0	-0.14612	0	135084443787
12	0	0	0	0	0	0	0	0	-0.17296	0	-0.15984	43534.72	0	0	-0.17445	164842795024
13	0	0	0	0	0	0	0	0	0	-0.21055	0	0	47836.31	-0.14612	0	181128112321
14	0	0	0	0	0	0	0	0	0	0	-0.15984	0	-0.21433	32613.22	-0.17445	123489396619
15	0	0	0	0	0	0	0	0	0	0	0	-0.19506	0	-0.14612	38935.2	147424467929

Table 24. *Test pressure in a six day of experiments*

15.099065879	15.099370115	15.099184173
15.099384384	15.099673570	15.099293887
15.099418094	15.099599617	15.099442827
15.099402435	15.099700000	15.099364533
15.099193557	15.099452995	15.099182667

For the pressure calibration coefficients P_{cb5} and P_{cb6} where the values of the block with the maximum is already below 15.10 bar, extrapolation was used following the trend resulting from the first 4 (P_{cb1} ... P_{cb4}).

The device readings from well 4 blank are shown in Table 25. The device was set to the maximum precision of 5 decimal places. The centralized values of the pressure evolution on the blocks are presented in Table 26.

Table 25*. Variation of reservoir pressure at well 4 during the experiment*

Time, days	***Pressure, bars***
0	15.100000
1	15.100010
2	15.100000
3	15.099999
4	15.099998
5	15.099996
6	15.099995

Studying Table 26 and the graph in Figure 7, we can see a progressive unloading of the blocks. The most apparent pressure drops are for blocks 1, 6, and 14, which have harmful sources (wells with production). The drop at block 15 is probably due to the need for a finer grid system that eliminates the interference between blocks 14 and 15.

It is also interesting to note the interconnectivity of blocks 5, 8, and 11 with the neighborhoods. Their high values between productive blocks indicate that their connectivity with neighboring blocks is not optimal.

The pressure variations are quite small at the devices' measurement limit. For a deeper analysis of the blocks' connectivity, it is necessary to extend the experiment over a much longer period, which was not possible for economic reasons.

The final step of the experiment, which also validates the modeling presented in the paper, is estimating the pressure variation in control well no. 4 from block ten resulting from the numerical modeling. These modeled values are compared with the reading of the depth manometer device from well 4.

Table 26 *Centralization of the pressure variation on the blocks resulted from numerical modeling*

pressure, bar	t=0	day 1	day 2	day 3	day 4	day 5	day 6
Bloc 1	15.100000	15.099998	15.099975	15.099921	15.099819	15.099345	15.099066
Bloc 2	15.100000	15.100000	15.099989	15.099961	15.099908	15.099517	15.099370
Bloc 3	15.100000	15.100000	15.099982	15.099939	15.099856	15.099414	15.099184
Bloc 4	15.100000	15.100000	15.099989	15.099963	15.099912	15.099525	15.099384
Bloc 5	15.100000	15.100000	15.099999	15.099997	15.099993	15.099685	15.099674
Bloc 6	15.100000	15.099999	15.099984	15.099949	15.099884	15.099473	15.099294
Bloc 7	15.100000	15.100000	15.099990	15.099967	15.099921	15.099544	15.099418
Bloc 8	15.100000	15.100000	15.099997	15.099988	15.099972	15.099644	15.099600
Bloc 9	15.100000	15.100000	15.099991	15.099969	15.099928	15.099557	15.099443
Bloc 10	15.100000	15.100000	15.099990	15.099965	15.099917	15.099535	15.099402
Bloc 11	15.100000	15.100000	15.100000	15.100000	15.100000	15.099700	15.099700
Bloc 12	15.100000	15.100000	15.099989	15.099960	15.099906	15.099514	15.099365
Bloc 13	15.100000	15.100000	15.099828	15.099940	15.099858	15.099419	15.099194
Bloc 14	15.100000	15.100000	15.099990	15.099969	15.099929	15.099562	15.099453
Bloc 15	15.100000	15.099999	15.099824	15.099939	15.099855	15.099413	15.099183

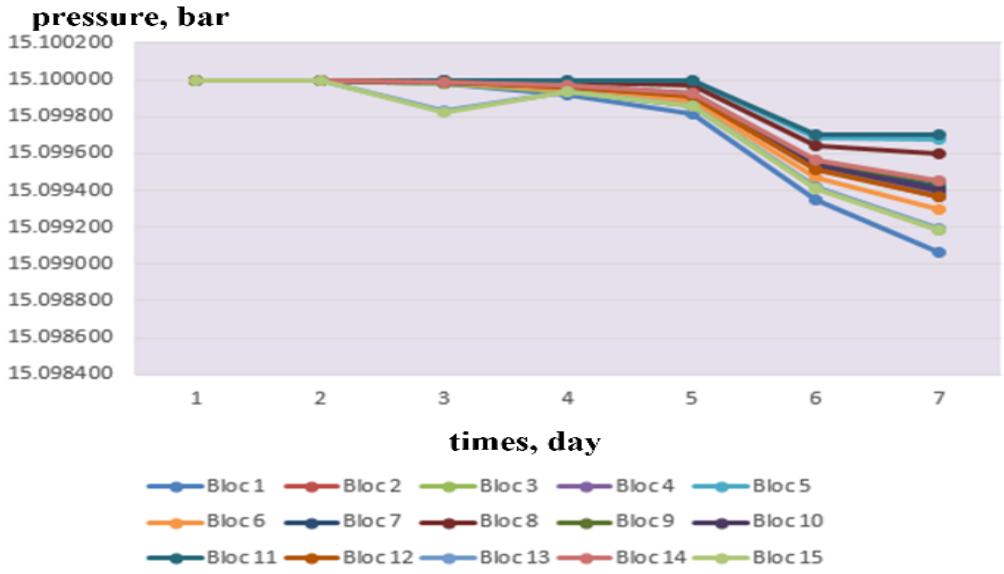

Figure 7*. Variation of modeled pressures on blocks*

The results of the comparison are shown in the graph in Figure 8. We notice that the two sets of values are correlative; their differences are close to the limit of the measuring devices' precision.

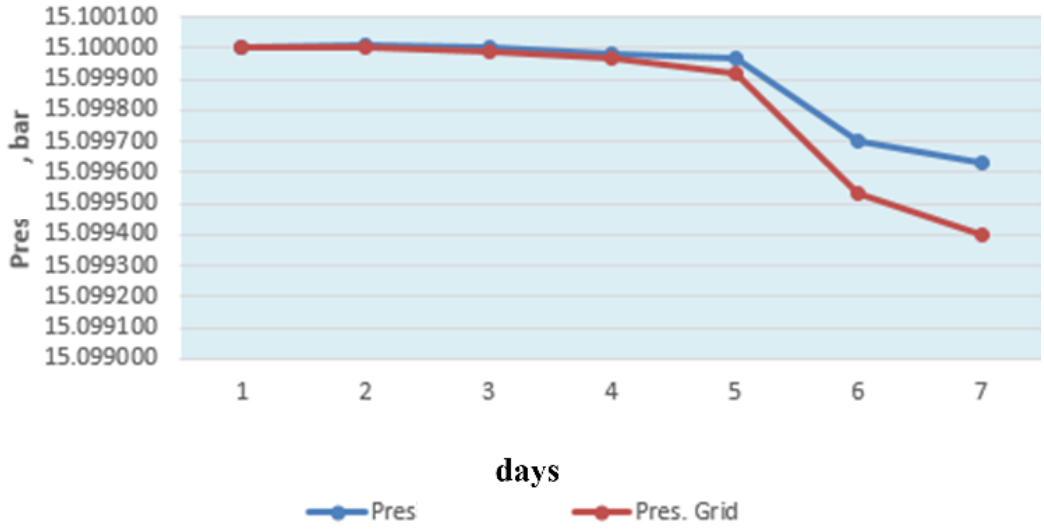

***Figure 8**. Comparison of pressure variation between modeling (grid pressure) and measurement from blank well 4*

CONCLUSIONS

The present paper, through the theoretical model presented, applied to a free gas field in the Transylvanian basin, aimed to build a theoretical framework through which the behavior of the depleted field can be followed by discretizing the field and setting some discrete properties (in the case present the deposit pressure), which by expanding the modeling can serve to identify poorly drained areas, which can be exploited in the future, contributing to the increase of the final recovery factor.

This discretization was achieved through the system of grid blocks, for which the average properties (temperature, pressure, permeability, etc.) and connectivity between them were modeled through the flow coefficients. The mathematical solution of the system of equations for a relatively short period of time due to economic considerations (6 days, closing the wells beyond this period was uneconomical) contributed significantly to the presentation of a theoretical model applied to the particular deposit, which can be extended for future production provisions, by setting time intervals e.g. to a month/year instead of days and extending the grid over the entire surface of the field, not only for the central area, where the wells are grouped.

Future experimental extensions, to more extensive deposits, for longer periods, will always be closely related to economic factors, being shutdowns on productive deposits. However, it must also be taken into account that the results of numerical modeling can bring benefits in the knowledge of the field, which can later materialize in economic benefits.

REFERENCES

[1] Avram L., Lupu D.A., The energy potential of natural gas fields from Transylvanian Basin: current and future trends, EMERG: Energy. Environment. Efficiency. Resources. Globalization, vol. 5, iss. 9, pp.156-162, 2019.

[2] Lupu D.A., Avram L., Improving the productivity of gas wells by stimulating "tight" formations – perspectives for continuation of exploitation in Transylvania basin, MATEC Web Conf. 342, 02001, 2021, DOI: 10.1051/matecconf/202134202001

[3] Dake L.P., Fundamentals of reservoir engineering. Shell International Petroleum Maatschappij, Haga, 1978

[4] Lee J., Wattenbarger R.A., Gas Reservoir Engineering, SPE Houston, Texas, 2004

[5] Tataru A., Sutoiu F., Balazs S., Mature Gas Fields Rehabilitation Concepts, AGH Drilling, Oil, Gas, Vol.31, No.2, p. 253-260, 2014

[6] Dumitrache L.N., Suditu S., Ghetiu I., Pana I., Branoiu G., Eparu C., Using Numerical Reservoir Simulation to Assess CO2 Capture and Underground Storage, Case Study on a Romanian Power Plant and Its Surrounding Hydrocarbon Reservoirs. Processes. 11(3):805. 2023

[7] Eparu C.N., Prundurel A.P., Doukeh R., Stoica D.B., Ghețiu I.V., Suditu S., Stan I.G., Rădulescu R., Optimizing underground natural gas storage capacity through numerical modeling and strategic well placement. Processes 2024, 12, 2136. https://doi.org/10.3390/pr12102136

[8] Prundurel A.P., Stan I.G., Pana I., Eparu C.N., Stoica D.B., Ghetiu I.V., Production forecasting at natural gas wells. Processes. 12(5):1009. 2024, https://doi.org/10.3390/pr12051009

[9] Helstern M., Sfiriac L., Stoicescu M., Reservoir optimisation of oil production by IPR curves, Chimia, 30th of May – 1st of June 2024, Constanta, Romania, Ovidius University Press, Constanta, 2024

[10] Stoica-Negulescu E.R., Biogenic accumulations in Romanian petroleum systems, AAPG Search and Discovery Article #90099 (2009), AAPG European Region Annual Conference Paris-Malmaison, France, November 2009, pp. 137-140

[11] Branoiu G., Frunzescu D., Nistor I., Jugastreanu C., Lungu I.A., Is there a future for oil and gas exploration in Romania ?, Proceedings of Geolinks International Conference on Geosciences, 1st edition, Athens, Greece, vol.1, pp. 183-191, 2019

[12] Ciupagea D., Pauca M., Ichim T., Geologia Depresiunii Transilvaniei, Editura Academiei RSR, Bucuresti, 1970.

[13] Cătuneanu O., Sequence stratigraphy of clastic systems: concepts, merits, and pitfalls, Journal of African Earth Sciences, 35, (2002), 1-43, 2002

[14] https://www.esri.com/partners/schlumberger-informa-a2T70000000TNdcEAG/petrel-e-p-software--a2d70000000VTIQAA4/

[15] Avram L., Lupu D.A., The influence of technological problems of the wells on the energy potential of the natural gas fields. EMERG: Energy. Environment. Efficiency. Resources. Globalization, vol. 8, iss. 1, pp.62-74, 2022.

[16] Helstern M., Bârsan D., Sandu T., Efficiency of polymer treatment of deposits to increase the ultimate recovery factor, 75 Years of Energy and Performance in Education and Research. Renewable Versus Fossil Fuels, Book of abstracts, Editura Universitatii Petrol-Gaze din Ploiesti, 2023, ISBN 978-973-719-887-7

Received:December 2024; Revised:December 2024; Accepted:December 2024; Published:December 2024